A new preconditioner for the EFIE based on primal and dual graph laplacian spectral filters

Material Strength and Applied Mechanics
A. Khotsianovsky and Y. Chen (Eds.)

doi:10.3233/ATDE240552

Numerical Modeling of Multi-Pass Arc Welding Processes: Integration with Experimental Validation for Distortion Analysis and Characterization

Péter GRUBITS[a], Rafaelle CUCUZZA[b], Dániel GOSZTOLA[a], Marco DOMANESCHI[b], János SZÉP[a], Majid MOVAHEDI RAD[a,1]
[a] *Department of Structural and Geotechnical Engineering, Széchenyi István University, H-9026 Győr, Hungary*
[b] *Department of Structural, Building and Geotechnical Engineering, Politecnico Di Torino, Corso Duca degli Abruzzi, 24 - 10129 Torino, Italy*
ORCiD ID: Majid Movahedi Rad https://orcid.org/0000-0002-8393-724X

Abstract. The increasing significance of numerical simulations in the welding industry arises from their capacity to improve manufacturing conditions, ensuring greater effectiveness and precision. The utilization of the finite element method (FEM) enables comprehensive and focused calculations of mechanical and material structural alterations induced by the welding process. Acquiring knowledge of these parameters not only serves to augment the quality of the manufacturing process but also yields consequential benefits, such as reducing adverse effects like base plate distortion. Consequently, enhancing structural performance and prolonging lifespan becomes achievable, aligning with overarching sustainability goals. To accomplish this objective, this paper involves the numerical simulation of a welding process based on experimental tests, with a focus on investigating the deformations caused by the heat generated during welding as the primary parameter of interest. Advanced modeling techniques are employed to assess the results as part of a comprehensive thermo-mechanical analysis framework, examining and characterizing the impact of the temperature distribution. In the finite element analysis (FEA), a total of 12 welding cycles were systematically modeled to align with experimental conditions, incorporating cooling intervals and preheating considerations. The outcomes of this research exemplify the potential of numerical simulation in the welding industry, demonstrating a diverse range of results achieved through FEA to enhance the quality of structures.

Keywords. FEM, welding simulation, multi-pass welding process

1. Introduction

The behavior of structures is significantly influenced by changes in ambient temperature. [1,2]. Therefore, it is essential to investigate the substantial heat generated during welding and its subsequent effects to improve the usability and extend the design lifespan of structures. Employing complex design methodologies such as the finite element

[1] Corresponding Author: Majid Movahedi Rad, E-mail: majidmr@sze.hu

method (FEM) can assist in simulating the entire welding process and accurately determining various mechanical and thermal parameters. [3].

This technique offers an extensive thermomechanical analysis and serves as an excellent tool for welding simulation [4]. Since the 1970s, this approach has been employed to model mechanical issues in welding processes. A significant milestone was achieved through the research conducted by Ueda and Yamakawa, who developed a method for theoretical analysis of the problem incorporating changes in temperature distribution over time and their impact on the mechanical properties of the material [5]. Another notable contribution in the early phase of welding simulation is the pioneering work of Goldak et al., where they integrated heat transfer, microstructure evolution, and thermal stress analysis [6]. Furthermore, Runnemalm made significant advancements in enhancing the efficiency of welding simulation in his dissertation, with a particular emphasis on multi-pass welding [7].

In the structural construction industry, plates often have relatively large thicknesses, requiring the formation of the final weld through multiple processes to establish a connection between them. Consequently, welding must be conducted in multiple stages, each characterized by different thermal cycles, which can have significant implications. Recent research has focused on the effects of multi-pass welding procedures, incorporating the analysis of out-of-plane distortion, residual stresses, and temperature variations [8–11].

In this study, the multi-pass welding process of two 20mm plates was simulated, conducting a comprehensive thermomechanical analysis over 12 cycles. The resulting temperatures were validated through experimental tests, followed by a parametric study of plate thickness commonly used in the construction industry, focusing on distortion. Advanced modeling techniques were employed to accomplish this objective, as detailed in this work.

2. Finite element model and analysis

2.1. Principle of the thermal analysis

Thermal analysis, grounded in the principles of heat transfer theory, is crucial in finite element simulations for the welding process. This method relies on the flux of energy [4], defined in Eq. (1) as follow:

$$q = -\kappa \nabla T \tag{1}$$

where the κ denotes the material characteristic and ∇T stands for the temperature variation. The flux of energy is directly influenced by thermal conductivity, which is the key element to calculate the temperature at each node utilizing the Eq. (2) [4] formulated as:

$$\frac{dh}{dt} + \nabla q + Q = 0 \tag{2}$$

where, Q is corresponding to the source of the heat generation, q denotes the heat flux vector, ∇ is the spatial gradient operator and t denotes the time. Additionally, the symbol h represents the energy per unit, referred to as specific heat enthalpy. The

increase in specific enthalpy under constant pressure for a slight change in temperature expressed in Eq. (3) [4]:

$$dh = c_p dT \tag{3}$$

where the c_p represents the specific heat capacity of the material, and dT is an increment in temperature.

In this research, the double ellipsoidal heat source model, commonly utilized for arc welding and developed by Goldak et al. [12], was applied to simulate the heat generated during welding, as depicted in Eqs. (4) and (5). Within the front and rear quadrants, the power density distribution q is given as:

$$q(x,y,z,t) = \frac{6\sqrt{3}f_f Q}{abc\pi\sqrt{\pi}} e^{-3x^2/a^2} e^{-3y^2/b^2} e^{-3z^2/{c_f}^2} \tag{4}$$

$$q(x,y,z,t) = \frac{6\sqrt{3}f_r Q}{abc\pi\sqrt{\pi}} e^{-3x^2/a^2} e^{-3y^2/b^2} e^{-3z^2/{c_r}^2} \tag{5}$$

where the width, depth, and length of the welding pool are determined by the parameters a, b, and c, representing the various axes of the ellipsoid aligned with the coordinate x, y, and z, respectively. Furthermore, the terms f_r and f_f represent the fraction factors of the heat, with the condition that $f_r + f_f = 2$, while Q denotes the energy input, formulated as:

$$Q = \eta UI \tag{6}$$

where I indicates the welding current, U represents the voltage, and η signifies the efficiency of the welding procedure. In this research, the analysis employs parameters provided in Table 1.

Table 1. Parameters of the heat source

Parameter	Value	Unit
Width of the heat source	2.00	mm
Depth of the heat source	2.00	mm
Front length of the heat source	2.50	mm
Rear length of the heat source	5.00	mm
Welding current	260.00	A
Welding voltage	23.00	V
Welding efficiency	0.60	-

To address the differential equation of the heat transfer theory, natural boundary condition has been established, expressed with the following formula [12]:

$$\kappa_n \frac{dT}{dn} + q + h(T - T_0) + \sigma\varepsilon\left(T^4 - {T_0}^4\right) = 0 \tag{7}$$

where κ denotes the thermal conductivity along the surface normal direction, q represents the prescribed flux, h stands for the heat transfer coefficient for convection, σ responds to the Stefan-Boltzmann constant, ε is the emissivity, and T_0 signifies the external temperature for convection and radiation. The variables utilized during the simulation are listed in Table 2.

Table 2. Coefficients for thermal properties

Coefficient	Value	Unit
Thermal conductivity normal to the surface	20.00	W/m^{2}K
Coefficient for convection	100.00	W/m^{2}K
Coefficient for emission	0.60	-

2.2. Principles of the mechanical analysis

Another crucial aspect in modeling welding operations is the mechanical analysis. The variation in heat distribution resulting from welding induces substantial expansions and contractions in the material. This leads to significant stresses arising from the thermal strains of the material [13].

Conducting thermal stress analysis and determining nonlinear deformations requires fundamental formulations including equilibrium equations, constitutive equations, and compatibility equations [4]. Utilizing the von Mises yield criterion and a standard elasto-plastic material model, the displacement field is interpolated over simulation-defined elements to solve these relationships, as follows [14]:

$$ {}^{n+1}_{i}u({}^{n+1}_{i}x, t) = N_m({}^{n+1}_{i}x)\,{}^{n+1}_{i}u(t) \tag{8} $$

where $N_m({}^{n+1}_{i}x)$ is the matrix containing the interpolation and shape function, while ${}^{n+1}_{i}u$ denotes the current estimation of the element displacement vector upon completion of the increment, with its corresponding coordinate being ${}^{n+1}_{i}x$.

2.3. Finite element model and analysis

In this research, a comprehensive 3D model of a lap-joint specimen was constructed, meticulously designed from two steel plates. The Finite Element model was carefully crafted to replicate the significant section of the experimental setup, which includes a flange plate of an I-beam measuring 360x80x20mm (depicted in white) and a stud plate of a steel-concrete composite bridge measuring 300x80x20mm (depicted in green). Both parts are constructed from the same grade of structural steel to ensure consistent material quality. To accurately represent the boundary conditions, a segment of the I-beam's web (red part) was integrated into the model. During the simulation, these components were joined by welding on both sides of the 80mm section. The overall size of the weld pool was set to 8mm, formed through 6 phases in the specified order as illustrated in Figure 1. This assembly was used for both the temperature validation of the experimental test and for the subsequent parametric study.

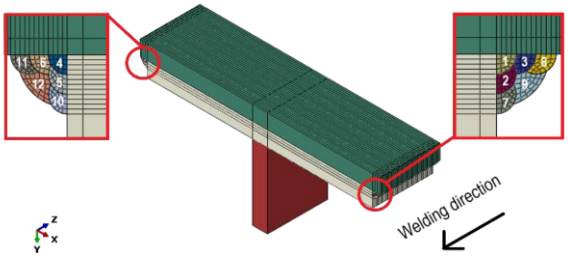

Figure 1. 3D finite element model

The simulation was conducted using ABAQUS software, wherein a coupled temperature-displacement analysis was performed [15]. In this instance, both thermal and mechanical solutions are derived simultaneously. Thus, it is imperative for the type of elements and the degree of freedom to remain consistent.

3. Results of the simulations

3.1. Results of the temperature validation

In the initial section of the research, the primary objective was to verify the temperatures recorded during the experimental tests. To enhance the quality of the weld pool and attain the most efficient connection feasible, the plates were preheated to 100 C°. According to the welding stages and considering the total welding time, the simulation duration was 723 seconds, encompassing the corresponding cooling period. During both the experimental test and the simulation, the temperature distribution was assessed on the opposite surface of the stud plate, precisely within the plane defined by the pool axis and the plate thickness. In the former case, these parameters were measured at specific time in each welding cycle, providing discrete data points.

Upon completion of the thermo-mechanical analysis, the temperature data from the simulation was compared to the results obtained from the experimental test. As illustrated in Figure 2, the temperatures derived from the model closely corresponded to those observed in the experiment. Specifically, the peak temperature recorded during the experimental test was 186°C, while the numerical simulation yielded a maximum of 180°C, with a deviation of less than 5%.

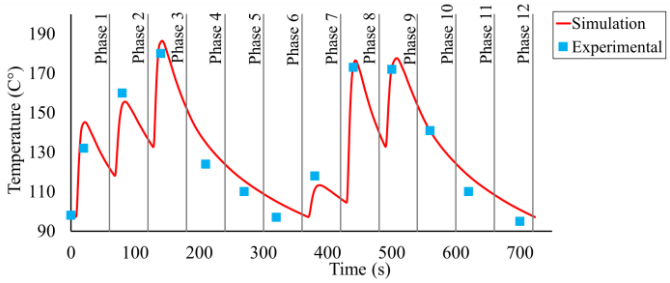

Figure 2. The temperature evolution in the specified measuring point

3.2. Results of the parametric study

After validation, a parameter study was conducted on the introduced numerical model to investigate the impact of plate thickness on resulting deformations. To accomplish this objective, five additional simulations were executed using the same variables as those employed previously. In this framework, the thickness of the plates under consideration was varied between 10mm and 20mm in 2mm increments. The deformations observed in the section perpendicular to the welding direction, captured at the middle of the longitudinal length of the plates after 12 welding cycles, are delineated in Figure 3. The points chosen for illustrating the distortion are aligned with the mesh of the numerical

model. Consequently, nodes along the inspected path, positioned on the underside of the stud plate and the top side of the flange plate of the specified section, were utilized.

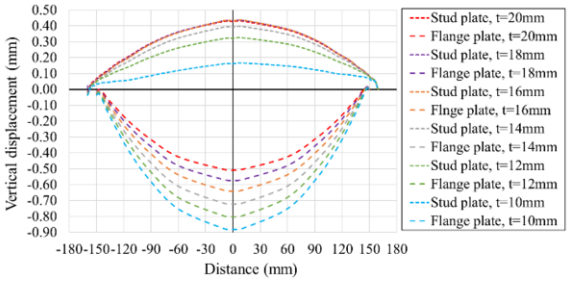

Figure 3. The deformations of the plates in the plane perpendicular to the welding direction.

The results indicate that reducing the plate thickness does not significantly alter the relative distance between the stud plate and the flange plate. However, it is noteworthy that as the plate thickness increases, the distortion of the flange plate decreases as expected, almost directly proportional to the increase, showing a 69.4% rise in distortion between 10mm and 20mm thick plates. In contrast, the distortion of the stud plate initially rises before stabilizing, maintaining near constancy. These relationships are illustrated in Figure 4.

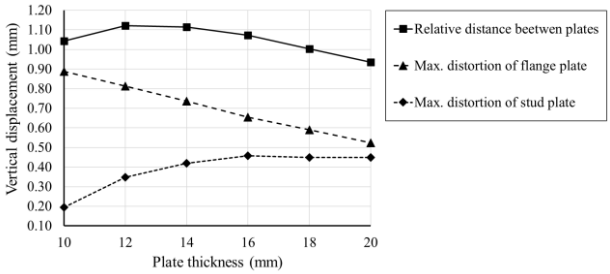

Figure 4. Deformations as a function of plate thickness

4. Conclusions

In this research, a numerical simulation of a multi-pass welding process involving two steel plates with relatively large thickness was introduced. The simulation employed a comprehensive coupled thermo-mechanical analysis, encompassing preheating of the configuration, 12 welding cycles, and cooling intervals. The resulting temperature distribution was validated through experimental tests, with the deviation of the peak temperature falling within 5% of the expected value.

In the subsequent phase of the research, a parametric study was conducted based on the previously established numerical model. The primary objective of this phase was to determine the influence of the plate thickness on the displacement caused by welding heat. To achieve this goal, five additional simulation was performed employing the relevant properties of the validated setup. The outcomes of this investigation revealed the correlation between plate thickness and welding-induced distortion. It was observed

that the alteration in the tested parameter predominantly impacted the thickness of the flange plate in the assembly, showing a 69.4% increase between plate thicknesses of 10mm and 20mm.

Our study establishes the groundwork for future exploration in this domain and contributes to the ongoing discussion surrounding welding methodologies. Subsequent investigations could build upon these findings to elucidate the behavior and capabilities of welded structures in greater detail.

References

[1] Habashneh M, Cucuzza R, Domaneschi M, Movahedi Rad M. Advanced elasto-plastic topology optimization of steel beams under elevated temperatures. Adv Eng Softw. 2024;190. doi:10.1016/j.advengsoft.2024.103596.
[2] Habashneh M, Rad MM. Reliability based topology optimization of thermoelastic structures using bi-directional evolutionary structural optimization method. Int J Mech Mater Des. 2023;19:605–20. doi:10.1007/s10999-023-09641-0.
[3] Grubits P, Dániel G, Habashneh M, Szép J, Rad MM. Advanced Numerical Simulation and Modeling of Welding Processes: Stochastic representation of parameters for Improved Fabrication. Chem Eng Trans 2023;107:619–24. doi:10.3303/CET23107104.
[4] Goldak JA, Akhlaghi Mehdi. Computational welding mechanics. Springer; 2005.
[5] Y. Ueda, T. Yamakawa. Analysis of Thermal Elastic-Plastic Stress and Strain During Welding by Finite Element Method. Trans Japan Weld Society 1971;2:90–100.
[6] Goldak J, Oddy A, Gu M, Ma W, Mashaie A, Hughes E, et al. Coupling Heat Transfer, Microstructure Evolution and Thermal Stress Analysis in Weld Mechanics Abstract. IUTAM Symposium on the Mechanical Effects of Welding, Springer-Verlag 1992:1–30.
[7] Runnemalm H. Efficient Finite Element Modelling and Simulation of Welding. 1999.
[8] Zhang Y, Tian L. The effect of joint configuration on residual stress and distortion of the 304 stainless steel multi-pass welded joints. Mater Today Commun 2022;30. doi:10.1016/j.mtcomm.2021.103070.
[9] Zubairuddin M, Albert SK, Vasudevan M, Mahadevan S, Chaudhari V, Suri VK. Numerical simulation of multi-pass GTA welding of grade 91 steel. J Manuf Process 2017;27:87–97. doi:10.1016/j.jmapro.2017.04.031.
[10] Vetriselvan R, Devakumaran K, Sathiya P, Ravichandran G. Transient out-of-plane distortion of multi-pass fillet welded tube to pipe T-joints. Defence Technol. 2017;13:77–85. doi:10.1016/j.dt.2016.06.002.
[11] Wang Y, Wang L, Di X, Shi Y, Bao X, Gao X. Simulation and analysis of temperature field for in-service multi-pass welding of a sleeve fillet weld. Comput Mater Sci. 2013;68:198–205. doi:10.1016/j.commatsci.2012.10.025.
[12] Goldak J, Chakravarti A, Bibby M. A New Finite Element Model for Welding Heat Sources. Metall Mater Trans B. 1984;15:299-305. doi: 10.1007/BF02667333
[13] Anca A, Cardona A, Risso J, Fachinotti VD. Finite element modeling of welding processes. Appl Math Model 2011;35:688–707. doi:10.1016/j.apm.2010.07.026.
[14] Lars-Erik L. Computational Welding Mechanics: Thermomechanical and Microstructural Simulations. Woodhead; 2007.
[15] Michael Smith. ABAQUS/Standard User's Manual, Version 6.9, 2009.